

Tube-based Nonlinear MPC of an Over-actuated Marine Platform for Navigation and Obstacle Avoidance using Control Barrier Functions

Spyridon Syntakas and Kostas Vlachos, *Member, IEEE*

Abstract—This paper presents the design of a robust tube-based nonlinear Model Predictive Control (MPC) law for a triangular marine platform, that is over-actuated with three rotating jets. The goal is safe navigation and dynamic positioning of the platform under realistic wind and wave environmental disturbances, as well as real-time obstacle avoidance employing Control Barrier Functions (CBF) as constraints in the robust MPC strategy. Extensive Monte Carlo simulations have been conducted under a control allocation scheme, taking into account the actuator thrust and rotation dynamics, sensor noise, as well as additional state and input constraints. The simulation results show that the nonlinear controller ensures robust and safe navigation with obstacle avoidance and accomplishes accurate positioning of the floating platform at a given goal pose, while satisfying the actuator limits.

I. INTRODUCTION

Floating platforms are widely used in offshore oil and gas production, aquaculture and fish farming, in offshore renewable energy plants, [1], as research in-the-field laboratories [2] and in general as auxiliary systems in marine applications. A common task for these platforms is to navigate to a desired goal pose, where they must remain stationary. To accomplish this, an appropriate actuation system must be able to provide the necessary forces to cancel environmental disturbances, like wind, wave and current forces, while ensuring the fulfilment of the navigation objective.

Safe control of these platforms, and marine vessels in general, is a challenging control problem that is of great concern from a research to a business standpoint. The hydrodynamic effects that occur as well as rigid body dynamics render the platform dynamics nonlinear, thus nonlinear control schemes have to be applied. Usually, these marine platforms are designed with redundant actuation, making the system over-actuated. So the control commands have to be efficiently allocated to the actuators, using allocate schemes that respect the actuator dynamics and limitations. These characteristics of the above control problem point to optimization based controllers that can respect the constraints of the system by design. By transcribing the control problem to a nonlinear program with constraints, that can be solved online using appropriate optimization techniques, really efficient

*We acknowledge support of this work by the project “Dioni: Computing Infrastructure for Big-Data Processing and Analysis.” (MIS No. 5047222) which is implemented under the Action “Reinforcement of the Research and Innovation Infrastructure”, funded by the Operational Programme “Competitiveness, Entrepreneurship and Innovation” (NSRF 2014-2020) and co-financed by Greece and the European Union (European Regional Development Fund).

Spyridon Syntakas and Kostas Vlachos are with the Department of Computer Science and Engineering, University of Ioannina, 45110 Ioannina, Greece. (Email: {ssyntakas; kostasvl}@cse.uoi.gr)

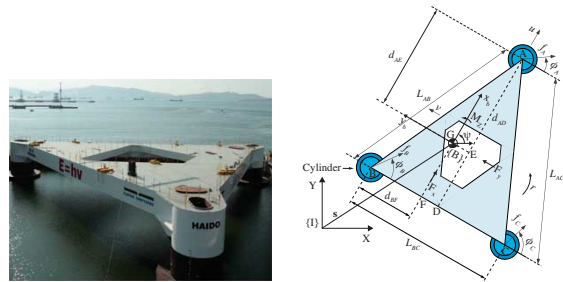


Fig. 1: The marine floating platform in-the-field and in a plan view

and elegant solutions can be formulated. Nonlinear Model Predictive Control (MPC) [3] is an approach that can tackle problems like the above, offering real-time control, while ensuring constraint satisfaction. Given that the environmental disturbances can be considered bounded, robust nonlinear MPC can be used to ensure the navigation and dynamic positioning of the platform. In addition, given the safety-critical aspect of the navigation of such a system, Control Barrier Functions (CBF) can be employed as constraints to the MPC to ensure robust real-time obstacle avoidance.

In recent years, MPC has been frequently used in marine vessel control and given the described complexity and nonlinearity of the problem, many flavors of MPC have been applied. A Lyapunov-based MPC strategy designed for dynamic positioning is used in [4] for an autonomous underwater vehicle and a nonlinear MPC law is used in [5] for motion control as well as thrust allocation of ships. To ensure robustness, tube-based MPC is used in [6] for the task of dynamic positioning of a ship, while [7] uses MPC for trajectory tracking for a fully-actuated surface vessel. Based on RCNNs, [8] designs an MPC law for tracking of under-actuated vessels, while an economic MPC strategy is presented in [9] with a trade-off between energy efficiency and safety. With regards to collision avoidance, [10] uses MPC and trajectory predictions based on RBF to accomplish multi-ship avoidance, while [11] is using CBFs to achieve reactive collision avoidance.

In this work, a tube-based nonlinear MPC strategy with CBFs is implemented for a marine platform, designed for the task of robust navigation and safe obstacle avoidance. The design of the tube-based controller follows the work presented in [12], where the uncertain system trajectories are forced by an ancillary MPC law to lie within a tube around a nominal trajectory derived using MPC on the certain system. Once robustness is ensured using Monte Carlo methods, CBFs are used as constraints, as in [13], to enable safe obstacle avoidance in a MPC-CBF manner. To our knowledge, this

is the first time that a CBF is employed as a constraint to a tube-based nonlinear model predictive controller of the form used in this work and the total hyperparameters of both the tube-based MPC strategy and the CBF are simultaneously tuned through stochastic simulations. Additionally, a nonlinear MPC law for dynamic positioning is used when the platform reaches a certain distance threshold from the goal pose. The inherent robustness of the nonlinear MPC law for dynamic positioning is proven through stochastic simulations and is able to stabilize the platform with minimal steady state error. The swap from the tube-based MPC navigation strategy to the nonlinear MPC law for dynamic positioning relaxes the computational burden of the platform's computational unit as the tube-based strategy requires the solution of two nonlinear programs simultaneously compared to the one nonlinear program required for the positioning controller. Altogether, the designed control scheme ensures the safe navigation of the marine platform and its accurate dynamic positioning despite the environmental disturbances. In [14], a robust MPC strategy with CBFs is presented for nonholonomic robots, aiming at obstacle avoidance with Input-to-State Stability and Input-to-State Safety theoretical guarantees. In comparison to our work, in [14] the constraint tightening is not done using stochastic simulations and the method is only aimed at nonholonomic robots.

II. DESCRIPTION OF THE MARINE PLATFORM

Initially designed to assist a deep-sea neutrino telescope, the marine platform is designed as an isosceles triangle with a mass of $425 \times 10^3 Kg$, actuated with three rotating diesel engine jets. At each corner of the platform exists a hollow double-cylinder in order to issue the necessary buoyancy. The three jets are placed inside the three hollow double-cylinders, where they rotate fully-submerged and parallel to the sea surface, using electro-hydraulic motors and can apply vectored thrust up to $20KN$. A detailed analysis of the design characteristics of the platform can be found in [15] along with a model-based PID controller for dynamic positioning. Other works, include a backstepping controller [16] and a linear MPC method [17] both designed for the task of dynamic positioning. Reinforcement Learning approaches has also been studied for the navigation of the platform, [18].

A. Kinematics

The planar kinematics of the platform are described by (1). The variables x, y, θ denote the position and orientation of the platform's fixed-body frame $\{B\}$ with respect to the inertial frame $\{I\}$, as depicted in Fig. 1. The fixed-body frame $\{B\}$ originates at the platform's center of mass (CM) located at point G . The variables u, v, r denote the surge and sway velocities and the yaw of the platform with respect to the fixed-body frame $\{B\}$. Control of the platform along the heave axis and about the roll and pitch axes is out of the scope of this work.

$${}^I \dot{\mathbf{x}} = \begin{bmatrix} \dot{x} \\ \dot{y} \\ \dot{\theta} \end{bmatrix} = \begin{bmatrix} \cos \theta & -\sin \theta & 0 \\ \sin \theta & \cos \theta & 0 \\ 0 & 0 & 1 \end{bmatrix} \begin{bmatrix} u \\ v \\ r \end{bmatrix} = {}^I R_B {}^B \mathbf{v} \quad (1)$$

B. Dynamics

Considering the platform dynamics, three distinct forces are accounted acting on the CM. These forces are the total control forces/torque from the three pump-jets, the hydrodynamic forces resulting from the cylinder motion w.r.t. the water and the forces due to environmental disturbances.

In Fig. 1, J_A, J_B, J_C denote the magnitude of the vectorized thrust each pump-jet provides, while ϕ_A, ϕ_B, ϕ_C denote the corresponding direction of each thrust. These thrusts provide the resultant forces $f_{c,x}, f_{c,y}$ that act on the platform's CM and the resultant torque $n_{c,z}$ around the vertical axis z_b that are used as virtual control inputs. The resultant forces and torque, contained in ${}^B \mathbf{q}_c$, are derived via the following linear operator,

$${}^B \mathbf{q}_c = \begin{bmatrix} f_{c,x} \\ f_{c,y} \\ n_{c,z} \end{bmatrix} = \begin{bmatrix} 1 & 0 & 0 \\ 0 & -1 & -d_{AG} \\ 1 & 0 & -d_{DC} \\ 0 & -1 & d_{DG} \\ 1 & 0 & d_{DC} \\ 0 & -1 & d_{DG} \end{bmatrix}^T \begin{bmatrix} J_A \sin \phi_A \\ J_A \cos \phi_A \\ J_B \sin \phi_B \\ J_B \cos \phi_B \\ J_C \sin \phi_C \\ J_C \cos \phi_C \end{bmatrix} = B {}^B \mathbf{f}_c \quad (2)$$

with the parameters in matrix B corresponding to geometric characteristics of the platform depicted in Fig. 1(b). The designed controller provides the virtual forces and torque acting on the CM, that can be allocated to the pump-jets using the Moore-Penrose inverse as ${}^B \mathbf{f}_c = B^\dagger {}^B \mathbf{q}_c$, in the case that the mean norm solution is enough and no additional requirements should be honored in virtual force allocation. This way the allocation is derived as:

$$J_k = \sqrt{(f_k \sin \phi_k)^2 + (f_k \cos \phi_k)^2}, \quad (3)$$

$$\phi_k = \arctan 2(J_k \sin \phi_k, J_k \cos \phi_k) \text{ for } k = \{1, 2, 3\}. \quad (4)$$

The hydrodynamic force that acts on the CM of the platform is derived as the total of the forces acting on each cylinder, i.e., added mass force and drag force. For a detailed analysis of hydrodynamics see [19]. The total forces acting on the CM due to rotational velocity of the platform are:

$${}^B \mathbf{q} = [m_a(2d_{AD} - 3d_{AE})r^2, m_a(\frac{3}{2}L_{BC} - 3d_{BF})r^2, 0]^T \quad (5)$$

with $m_a = -C_\alpha \pi \rho [R_{uc}^2(H_{uc} + R_{lc}^2 H_{lc})]$, where C_α is the added mass coefficient, ρ is the water density and R_{uc}, H_{uc}, H_{lc} denote the radius and height of the upper cylinder and the height of the lower cylinder respectively.

Disturbance forces ${}^B \mathbf{q}_{dist}$ are acting on the platform's CM due water and wind environmental disturbances, ${}^B \mathbf{q}_{water}$ and ${}^B \mathbf{q}_{wind}$ respectively. The simulation of the disturbance forces/torque is based on [20] and calculated as

$${}^B \mathbf{q}_{dist} = {}^B \mathbf{q}_{water}^T + {}^B \mathbf{q}_{wind}^T \quad (6)$$

Disturbances coming from water consist of two terms. The first corresponds to forces depended on water speed and acceleration and the second corresponds to forces due to wave oscillation and wave drift. Wave oscillation is simulated as white Gaussian noise. Wind forces/torque and wave drift disturbances depend on wind velocity and magnitude that is

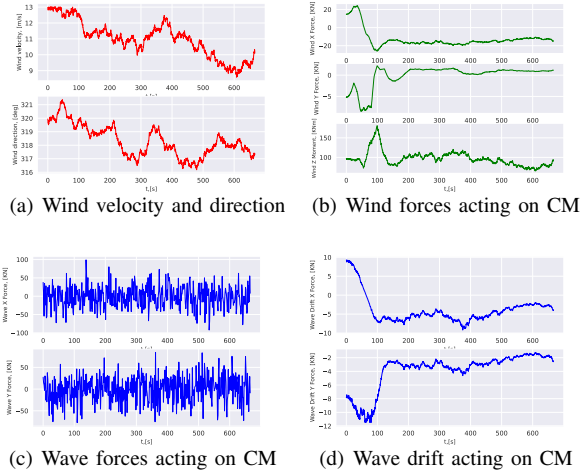


Fig. 2: Environmental disturbances taken from simulations.

simulated as integrated Gaussian noise, with maximum value at 4 *Beaufort*. Bounds on the disturbance values are based on meteorological data and an example of the disturbances used in the simulations can be seen in Fig. 2.

Based on the above forces/torques, the dynamic equation of motion of the platform w.r.t. the fixed-body frame $\{B\}$ is derived using first principles as:

$$M^B \dot{\mathbf{v}} = {}^B \mathbf{q} + {}^B \mathbf{q}_{dist} + {}^B \mathbf{q}_c \quad (7)$$

with the mass matrix $M = \text{diag}(m - 3m_\alpha, m - 3m_\alpha, m_{33})$ and $m_{33} = I_{zz} - (d_{AG}^2 + 2d_{BD}^2 + 2d_{DG}^2)m_\alpha$, where m denotes the mass of the platform and I_{zz} is its mass moment of inertia about the z_b axis, see Fig 1.

1) *Actuator Dynamics*: The ${}^B \mathbf{q}_c$ vector contains the virtual input forces acting on CM, as derived by the control system. These forces, as mentioned, are allocated to the pump-jets based on (2). The immediate application of the desired allocated thrust is not possible due to the pump-jets dynamics and limitations. The actuator dynamics are simply modeled as first order lags, as

$$\dot{J}_k = \frac{1}{\tau_J}(J_{k,des} - J_k) \text{ and } \dot{\phi} = \frac{1}{\tau_\phi}(\phi_{k,des} - \phi_k) \quad (8)$$

with τ_J , τ_ϕ denoting each jet's thrust and rotation time constants. The pump-jet's model is a lot more complex in reality, see [15] for more details, but the simplified first-order lag model is used in the simulation. The actuator limitations are also considered using the manufacturer sheets.

III. DESIGN OF THE ROBUST NONLINEAR MPC LAW

The design of the control system for the navigation of the platform is based on a tube-based nonlinear MPC [12], and obstacle avoidance is accomplished by employing a DCBF, [13]. For obstacle avoidance, we assume the presence of a perception system capable of real-time obstacle detection that can provide coordinates of obstacles with respect to a known frame, the design and implementation of which, is out of the scope of this work.

Starting from (7) and combining (1) and its derivative, ${}^B \dot{\mathbf{v}} = {}^I R_B^{-1} ({}^I \ddot{\mathbf{x}} - {}^I \dot{R}_B \mathbf{v})$ the open loop dynamics of the platform is described as

$${}^I \ddot{\mathbf{x}} = {}^I \dot{R}_B {}^I R_B^{-1} \dot{\mathbf{x}} + {}^I R_B M^{-1} ({}^B \mathbf{q} + {}^B \mathbf{q}_{dist} + {}^B \mathbf{q}_c) \quad (9)$$

By augmenting the model with the observed variables as $\mathbf{x}_{aug} = [x, y, \theta, \dot{x}, \dot{y}, \dot{\theta}]^T$, the open loop dynamic equation (9) takes the form of

$$\dot{\mathbf{x}}_{aug} = \begin{bmatrix} O_{3 \times 3} & I_{3 \times 3} \\ O_{3 \times 3} & {}^I \dot{R}_B {}^I R_B^{-1} \end{bmatrix} \mathbf{x}_{aug} + \begin{bmatrix} O_{3 \times 3} \\ {}^I R_B M^{-1} \end{bmatrix} ({}^B \mathbf{q} + {}^B \mathbf{q}_{dist} + {}^B \mathbf{q}_c) \quad (10)$$

with O and I denoting the zero and identity matrices respectively. This way the model takes the standard form of the disturbed nonlinear system, i.e.,

$$\dot{\mathbf{x}} = f(\mathbf{x}, \mathbf{u}) + \mathbf{w} \quad (11)$$

with \mathbf{x} denoting the augmented state vector \mathbf{x}_{aug} , \mathbf{u} the input vector ${}^B \mathbf{q}_c$ and \mathbf{w} the bounded disturbances. The equivalent certain system has the form

$$\dot{\mathbf{z}} = f(\mathbf{z}, \mathbf{v}) \quad (12)$$

with \mathbf{z} denoting the augmented state vector \mathbf{x}_{aug} and \mathbf{v} the input vector ${}^B \mathbf{q}_c$ for the certain system.

A. Robust Navigation

Robust navigation is ensured by forcing all the possible uncertain trajectories within a tube around a nominal trajectory. A nominal MPC law is designed using the deterministic system dynamics (12), that derives a desired state and input trajectory, that is used as reference. The feedback control signal for the disturbed system (11) is derived by an ancillary nonlinear MPC law that steers the trajectories of the disturbed system to the reference nominal trajectory. By tightening the constraint set of the nominal deterministic controller, robustness can be ensured, as the disturbed system trajectories are forced to be contained within a tube around the nominal trajectory.

1) *Nominal MPC*: If \mathbf{x}_{des} denotes a goal state for the disturbed system, the nominal MPC law, that provides the reference trajectory for the ancillary controller, is defined as

$$\min_{\mathbf{z}, \mathbf{v}} V_f(\mathbf{z}_{t+N|t} - \mathbf{x}_{des}) + \sum_{k=0}^{N-1} l(\mathbf{z}_{t+k|t} - \mathbf{x}_{des}, \mathbf{v}_{t+k|t}) \quad (13)$$

$$\mathbf{z}_{t+k+1|t} = f(\mathbf{z}_{t+k|t}, \mathbf{v}_{t+k|t}) \quad (14)$$

$$\mathbf{z}_{t+k|t} \in \mathcal{Z}, \mathbf{v}_{t+k|t} \in \mathcal{V} \quad (15)$$

$$\mathbf{z}_{t|t} = \mathbf{z}_t \quad (16)$$

$$\mathbf{z}_{t+N|t} = \mathbf{x}_{des} \quad (17)$$

for $k = \{0, 1, 2, \dots, N-1\}$, with N being the control horizon and $\mathbf{z}_{t+k|t}$ denoting the state vector at time $t+k$, predicted at time t , if $\mathbf{v}_{t:t+k-1|t}$ is applied to the system model from the current state \mathbf{z}_t . If $\mathbf{v}_{t:t+N-1}^* = (\mathbf{v}_{t|t}^*, \mathbf{v}_{t+1|t}^*, \dots, \mathbf{v}_{t+N-1|t}^*)$ is the optimal control trajectory, obtained by solving (13) at time t , then, only the first input is applied to the system leading to an MPC feedback control law of the form

$\mathbf{v}(t) = \mathbf{v}_{t|t}^*(\mathbf{z}_t)$. The nonlinear program is solved at each time step, leading to the receding horizon controller. In (13), $l(\mathbf{z}_{t+k|t} - \mathbf{x}_{des}, \mathbf{v}_{t+k|t})$ denotes the stage cost, while $V_f(\mathbf{z}_{t+N|t} - \mathbf{x}_{des})$ represents the terminal cost. The stage cost has the form $(\mathbf{z} - \mathbf{x}_{des})^T Q(\mathbf{z} - \mathbf{x}_{des}) + \mathbf{v}^T R \mathbf{v}$, with the weighting matrices Q and R defined as diagonal and positive definite. The terminal cost V_f together with the terminal equality constraint (17) are chosen as in [21] and [3] to satisfy the "stability axioms". V_f is determined in general as $\mathbf{z}^T P \mathbf{z}$ with P denoting the Lyapunov matrix, obtained by linearizing the model (7) at the equilibrium and solving the Algebraic Riccati Equation. Equation (14) describes the certain system dynamics. $\mathcal{Z} \in \alpha \mathcal{X}$ and $\mathcal{V} \in \beta \mathcal{U}$ are compact sets containing the equilibrium, i.e., $\mathbf{x}_{des} \in \mathcal{Z} \times \mathcal{V}$, and are tightened versions of the ancillary MPC constraint sets, \mathcal{X}, \mathcal{U} . The hyper parameters $\alpha \in (0, 1]$, $\beta \in (0, 1]$ are chosen via Monte Carlo simulations to ensure constraint satisfaction for the disturbed system.

2) *Ancillary MPC*: The ancillary nonlinear MPC defines the control law for the plant, i.e., the disturbed system (11). It is designed to drive the disturbed system on the nominal reference trajectory, thus its cost function is defined as the deviation between the reference nominal trajectory, i.e., $\mathbf{z}_{t:t+N}^* = (\mathbf{z}_{t|t}^*, \mathbf{z}_{t+1|t}^*, \dots, \mathbf{z}_{t+N|t}^*)$, $\mathbf{v}_{t:t+N-1}^* = (\mathbf{v}_{t|t}^*, \mathbf{v}_{t+1|t}^*, \dots, \mathbf{v}_{t+N-1|t}^*)$ at time t , and the state and control, $\mathbf{x}_{t:t+N}$, $\mathbf{u}_{t:t+N}$ trajectories of the disturbed system.

Thus, the ancillary MPC law is designed as

$$\min_{\mathbf{x}, \mathbf{u}} V_f + \sum_{k=0}^{N-1} l(\mathbf{x}_{t+k|t} - \mathbf{z}_{t+k|t}^*, \mathbf{u}_{t+k|t} - \mathbf{v}_{t+k|t}^*) \quad (18)$$

$$\mathbf{x}_{t+k+1|t} = f(\mathbf{x}_{t+k|t}, \mathbf{u}_{t+k|t}) \quad (19)$$

$$\mathbf{x}_{t+k|t} \in \mathcal{X}, \mathbf{u}_{t+k|t} \in \mathcal{U} \quad (20)$$

$$\mathbf{x}_{t|t} = \mathbf{x}_t \quad (21)$$

where the stage cost $l(\mathbf{x}_{t+k|t} - \mathbf{z}_{t+k|t}^*, \mathbf{u}_{t+k|t} - \mathbf{v}_{t+k|t}^*)$ is defined as $(\mathbf{x}_{t+k|t} - \mathbf{z}_{t+k|t}^*)^T Q(\mathbf{x}_{t+k|t} - \mathbf{z}_{t+k|t}^*) + (\mathbf{u}_{t+k|t} - \mathbf{v}_{t+k|t}^*)^T R(\mathbf{u}_{t+k|t} - \mathbf{v}_{t+k|t}^*)$ with Q, R designed as diagonal and positive definite matrices, penalizing the deviation. $V_f := V_f(\mathbf{x}_{t+N|t} - \mathbf{x}_{des})$ represents again the terminal cost and is used to ensure stability. In (20), \mathcal{X}, \mathcal{U} are the state and input constraint sets, while (19) describes the plant dynamics.

By solving this nonlinear program in every time step, the optimal input trajectory is derived as $\mathbf{u}_{t:t+N-1}^* = (\mathbf{u}_{t|t}^*, \mathbf{u}_{t+1|t}^*, \dots, \mathbf{u}_{t+N-1|t}^*)$. The first element is applied to the disturbed system defining the control law, $\mathbf{u}_t = \mathbf{u}_{t|t}^*$. This control law ensures robustness and stability and can drive the plant to the desired goal.

B. Tube MPC with DCBF for Safe Obstacle Avoidance

Barrier functions are employed to ensure forward invariance of a set and are used commonly in safety-critical control. A safe set \mathcal{C} is a super-level set of a function $h : \mathcal{X} \subset \mathbb{R}^N \rightarrow \mathbb{R}$ with $\mathcal{C} = \{\mathbf{z} \in \mathbb{R}^n : h(\mathbf{z}) \geq 0\}$ and $\partial \mathcal{C} = \{\mathbf{z} \in \mathbb{R}^n : h(\mathbf{z}) = 0\}$ and additionally in the interior of \mathcal{C} , the function h is always positive, [22]. For discrete

systems, if the condition

$$\Delta h(\mathbf{z}_k, \mathbf{v}_k) \geq -\gamma h(\mathbf{z}_k) \text{ for } \gamma \in (0, 1] \quad (22)$$

holds, then h is a Discrete Control Barrier function (DCBF) that renders the set \mathcal{C} safe. Intuitively, by starting within the safe set \mathcal{C} and by constraining the value of ∂h so that it never reaches infinity within \mathcal{C} , the set \mathcal{C} is rendered forward invariant. The hyperparameter γ acts on the decay rate of lower bound of the CBF, as it decreases with rate $1-\gamma$. Thus, a smaller choice of γ increases the safety of the system. A small γ on the other hand can render the optimization problem infeasible, as the safe set \mathcal{C} and the reachable set \mathcal{R} may not intersect, i.e., $\mathcal{C} \cap \mathcal{R} = \emptyset$. The choice of γ in this work is made w.r.t. to the safety and reachability aspects using Monte Carlo methods.

By employing an appropriate constraint in the form of (22) in the MPC formulation, safety-critical systems can be controlled with safety guaranties. For an in-depth study of nonlinear system safety control with discrete CBFs (DCBF) refer to [22]. For the tube-based nonlinear MPC that is studied in this paper, the DCBF of the form (23) for obstacle avoidance is employed as a constraint in the nominal MPC (13), that keeps the system in the safe set $\mathcal{C} = \{\mathcal{X} \setminus \mathcal{O}\}$, with \mathcal{X} denoting the admissible set of states of the disturbed system (11) and \mathcal{O} the obstacle space.

C. Dynamic Positioning

With regard to dynamic positioning, inherent robustness of an appropriately designed nonlinear MPC strategy is enough to robustly stabilize the disturbed system to a goal state, \mathbf{x}_{des} . The inherent robustness of appropriate designed controllers is also established in related works [17], [16], [15]. Thus, nonlinear MPC of the form (13) is designed for the task of dynamic positioning of the discretized disturbed model (11).

IV. SIMULATION RESULTS

A. Monte Carlo Simulations of Navigation

The robustness of the tube-based nonlinear MPC is established using Monte Carlo methods. The tightened constraint sets of the nominal MPC are chosen through extensive stochastic simulations, such that \mathbf{x} and \mathbf{u} always remain in the interior of \mathcal{X}, \mathcal{U} and the disturbed plant always converges to the desired goal state.

The platform was given several initial and goal states, for which it had to navigate to, commanded by the tube-based MPC. When the platform reaches a distance less than $5m$ from the goal position the tube-based MPC law is swapped to an MPC strategy designed specifically for dynamic positioning, as described in section III. The terminal constraint is omitted during dynamic positioning as \mathbf{x}_N always lies inside the terminal set \mathcal{X}_f by choosing an appropriate horizon length. The penalty matrices for the nominal MPC were set as $Q_{nom} = \text{diag}(10^3, 10^3, 10^6, 10^3, 10^3, 10^3)$ and $R_{nom} = \text{diag}(10^{-5}, 10^{-5}, 10^{-6})$ while the ancillary MPC deviation was penalized more intensively as $Q_{anc} = \text{diag}(10^8, 10^8, 10^{10}, 10^7, 10^7, 10^7)$ and $R_{anc} = \text{diag}(10^{-1}, 10^{-1}, 10^{-2})$ in order to ensure convergence of

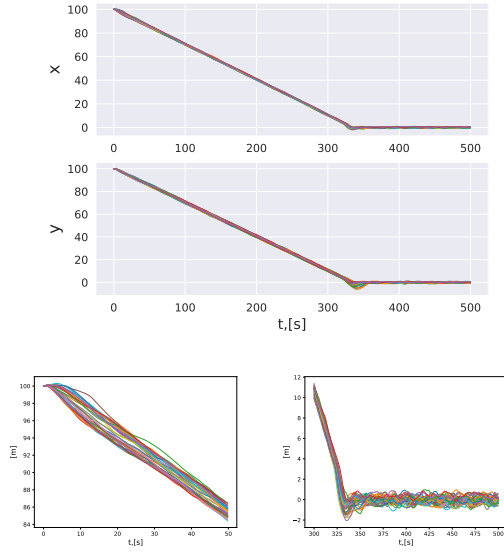


Fig. 3: (a) x,y state trajectories, (b) Tube close-up during navigation, (c) Close-up of trajectories during dynamic positioning

the ancillary MPC trajectories to the nominal reference trajectories. The MPC for the dynamic positioning has $Q_{dyn} = \text{diag}(10^7, 10^7, 10^7, 10^2, 10^2, 10^2)$ and $R_{dyn} = \text{diag}(10^{-3}, 10^{-3}, 10^{-4})$. The nonlinear controllers have been implemented using the CasADI framework for nonlinear optimization [23] by transcribing the optimal control problems into nonlinear programs using multiple shooting. IPOPT [24] is the solver of choice. The horizon is chosen as $N = 30$ and a time step of $T = 0.3\text{sec}$ is used for all MPC formulations.

Simulations of the closed-loop disturbed system begin from a random initial choice of tightening hyper-parameters, α, β . Noise of $\pm 1m$ and $\pm 5^\circ$ is added to the observed pose states, to account for GPS sensor noise. An initial bound of 15knots on the wind velocity is used, which also enforces bounds on wind and wave drift forces that act on the platforms CM. The final bound on disturbances, for which robustness holds, is determined from the stochastic simulations. The forces due to wave oscillation are simulated as white Gaussian noise with $std = 30KN$ throughout the simulations. For a given initial and goal state, a simulation cycle begins with the wind direction at 0° and is incremented by 10° with each simulation, leading to 36 simulations for each initial and goal state. The wind velocity, wind direction and wave drift force sequences are calculated based on random sampling according to the disturbance models. The results of each simulation cycle points to changes of the tightening hyper-parameter values α, β that lead to maximum spreads of the variables of interest such that the constraint sets are not violated. That way the final hyperparameter values are chosen after many simulation cycles. Visually, tubes begin to formulate around the nominal trajectories with appropriate deviations leading to safety and robustness. The variables of interest are the x, y position state variables and their spread around the nominal trajectory must form a tight tube. The actuation dynamics (8) and limitations are taken into account during the virtual force allocation throughout

the simulations.

After conducting the described Monte Carlo simulations, it is derived that for a 13knots bound on the wind velocity and choosing $\alpha = 0.4$ in order to tighten the constraints only on the $[\dot{x}, \dot{y}, \dot{\theta}]$ states, while $\beta = 1$, tubes like the ones depicted in Fig. 3 begin to formulate around the nominal trajectory. The tubes maintain the depicted deviation from the nominal trajectory throughout extensive stochastic simulations that are conducted using the above bounds. Thus, the choice of a tube-based nonlinear MPC designed as in section III and using the constraint tightening and disturbance bounds derived from Monte Carlo simulations, results in robust navigation of the platform. The nonlinear MPC that is used for the task of dynamic positioning, has the inherent robustness to stabilize the platform as it reaches the goal state as seen in Fig. 3 (c).

B. Obstacle avoidance with CBF

Once robustness has been established and the formulated tubes have appropriate maximum size with small deviation from the nominal trajectory, obstacle avoidance can be accomplished in a safety-critical manner by using a CBF as a constraint to the nominal MPC. Using the aforementioned tightened constraint sets and hyperparameters, a DCBF constraint of the form $\Delta h(\mathbf{x}_k, \mathbf{u}_k) \geq -\gamma h(\mathbf{x}_k)$ is used for obstacle avoidance with

$$h(\mathbf{x}_k) = \|\mathbf{x}_k - \mathbf{o}\|_2^2 - (d_s + r_o^2) \quad (23)$$

The variable r_o denotes the radius of circular space surrounding a perceived obstacle with position $[o_x, o_y]^T$. The hyper parameter γ is chosen as $\gamma = 0.3$ through stochastic simulations as the system remains safe and the optimization feasibility holds. d_s is a tightening variable of the safe set, that represents a bound on the distance the platform is allowed to have from the obstacle. d_s is set as $d_s = d_{AD} + \delta$, with d_{AD} being the height of the triangular platform and δ is a length margin equal to $7m$. Monte Carlo methods have been also applied to the system to verify the robust and safety-critical obstacle avoidance. An example of obstacle avoidance from a Monte Carlo simulation cycle is depicted in Fig. 4. Fig. 4 also depicts the x, y, θ state trajectories from one of these simulations along with the steady state error. The nonlinear MPC that is activated when the platform reaches the threshold of $5m$ from the goal state results to accurate dynamic positioning. Fig. 5 (a) depicts the output virtual forces of the controller that act on the CM and their corresponding allocation is depicted in Fig. 5 (b), (c).

V. CONCLUSION

The paper presents the design of a tube-based nonlinear MPC law aiming at safe and robust navigation of an over-actuated triangular floating platform with obstacle avoidance capabilities. An appropriate control allocation scheme is used in order to achieve task completion while honoring the dynamics and limitations of the actuation. Extensive Monte Carlo simulations were conducted under realistic actuator limit constraints and settling delays, as well as realistic environmental disturbances and sensor noise. Based on many

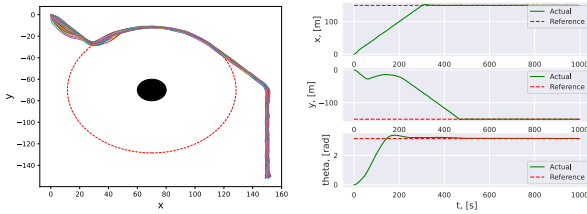


Fig. 4: (a) Paths followed while avoiding a static obstacle, under various bounded environmental disturbances for one simulation cycle. The black circle is an obstacle of radius $r_{obs} = 10m$. The red dash-dotted circle with radius $r = r_{obs} + d_s$ depicts the boundaries of the safe set \mathcal{C} , (b) x, y, θ trajectories with steady state errors $x_{error} = 0.26m$, $y_{error} = 0.008m$, and $\theta_{error} = 0.6^\circ$.

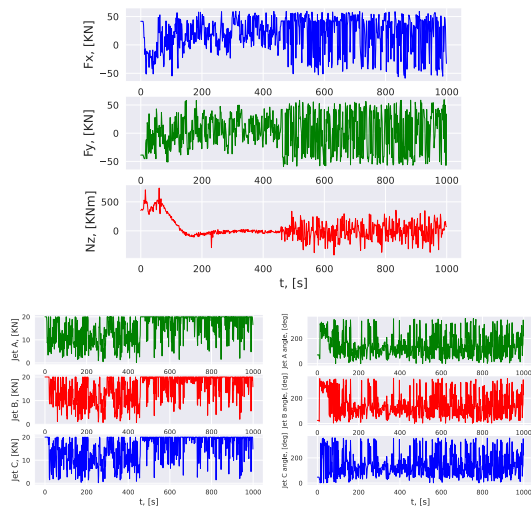


Fig. 5: (a) Input virtual forces $B \mathbf{q}_c$ on the CM respecting actuator dynamics and limitations, (b) Allocated pump-jet forces, (c) Angles of the pump-jets

sequential stochastic simulation cycles, the robustness and stability of the tube-based nonlinear MPC is ensured via appropriate tightening of the constraint sets, hyperparameter tuning and the use of appropriate terminal costs and constraints. The employed DCBF enhances the robust controller with safety-critical obstacle avoidance capabilities with feasibility guaranties. For the task of dynamic positioning the nonlinear MPC inherent robustness is enough to stabilize the platform with minor steady state error.

REFERENCES

- [1] K. P. Thiagarajan and H. J. Dagher, "A Review of Floating Platform Concepts for Offshore Wind Energy Generation," *Journal of Offshore Mechanics and Arctic Engineering*, vol. 136, no. 2, 03 2014, 020903. [Online]. Available: <https://doi.org/10.1115/1.4026607>
- [2] L. Pei, Y. Zhengdong, and J. Li, "Marine meteorological observation technology and application based on large floating platform," in *2019 International Conference on Meteorology Observations (ICMO)*, 2019, pp. 1–4.
- [3] D. Q. Mayne, "Model predictive control: Recent developments and future promise," *Automatica*, vol. 50, no. 12, pp. 2967–2986, 2014. [Online]. Available: <https://www.sciencedirect.com/science/article/pii/S0005109814005160>
- [4] C. Shen, Y. Shi, and B. Buckham, "Lyapunov-based model predictive control for dynamic positioning of autonomous underwater vehicles," in *2017 IEEE International Conference on Unmanned Systems (ICUS)*, 2017, pp. 588–593.
- [5] A. Bärlund, J. Linder, H. Feyzmahdavian, M. Lundh, and K. Tervo, "Nonlinear mpc for combined motion control and thrust allocation of ships," *IFAC-PapersOnLine*, vol. 53, no. 2, pp. 14 698–14 703, 2020, 21st IFAC World Congress. [Online]. Available: <https://www.sciencedirect.com/science/article/pii/S2405896320324472>
- [6] A. A. do Nascimento, H. R. Feyzmahdavian, M. Johansson, W. Garcia-Gabin, and K. Tervo, "Tube-based model predictive control for dynamic positioning of marine vessels," *IFAC-PapersOnLine*, vol. 52, no. 21, pp. 33–38, 2019, 12th IFAC Conference on Control Applications in Marine Systems, Robotics, and Vehicles CAMS 2019. [Online]. Available: <https://www.sciencedirect.com/science/article/pii/S2405896319321640>
- [7] L. M. Kinjo, S. Wirtensohn, J. Reuter, T. Menard, and O. Gehan, "Trajectory tracking of a fully-actuated surface vessel using nonlinear model predictive control: Experimental results," in *2022 30th Mediterranean Conference on Control and Automation (MED)*, 2022, pp. 693–698.
- [8] Z. Yan and J. Wang, "Model predictive control for tracking of under-actuated vessels based on recurrent neural networks," *IEEE Journal of Oceanic Engineering*, vol. 37, no. 4, pp. 717–726, 2012.
- [9] H. Liang, H. Li, J. Gao, R. Cui, and D. Xu, "Economic mpc-based planning for marine vehicles: Tuning safety and energy efficiency," *IEEE Transactions on Industrial Electronics*, pp. 1–11, 2022.
- [10] M. Papadimitrakis, M. Stogiannos, H. Sarimveis, and A. Alexandridis, "Multi-ship control and collision avoidance using mpc and rbf-based trajectory predictions," *Sensors*, vol. 21, no. 21, 2021. [Online]. Available: <https://www.mdpi.com/1424-8220/21/21/6959>
- [11] E. H. Thyri, E. A. Basso, M. Breivik, K. Y. Pettersen, R. Skjetne, and A. M. Lekkas, "Reactive collision avoidance for asvs based on control barrier functions," in *2020 IEEE Conference on Control Technology and Applications (CCTA)*, 2020, pp. 380–387.
- [12] D. Q. Mayne, E. C. Kerrigan, E. J. van Wyk, and P. Falugi, "Tube-based robust nonlinear model predictive control," *International Journal of Robust and Nonlinear Control*, vol. 21, no. 11, pp. 1341–1353, 2011. [Online]. Available: <https://onlinelibrary.wiley.com/doi/abs/10.1002/rnc.1758>
- [13] J. Zeng, B. Zhang, and K. Sreenath, "Safety-critical model predictive control with discrete-time control barrier function," in *2021 American Control Conference (ACC)*, 2021, pp. 3882–3889.
- [14] Y. S. Quan, J. S. Kim, and C. C. Chung, "Robust model predictive control with control barrier function for nonholonomic robots with obstacle avoidance," in *2021 21st International Conference on Control, Automation and Systems (ICCAS)*, 2021, pp. 1377–1382.
- [15] K. Vlachos and E. Papadopoulos, "Modeling and control of a novel over-actuated marine floating platform," *Ocean Engineering*, vol. 98, pp. 10–22, 2015. [Online]. Available: <https://www.sciencedirect.com/science/article/pii/S0029801815000207>
- [16] A. Tsopeidakis, K. Vlachos, and E. Papadopoulos, "Backstepping control with energy reduction for an over-actuated marine platform," in *2015 IEEE International Conference on Robotics and Automation (ICRA)*, 2015, pp. 553–558.
- [17] —, "Design of a linear model predictive controller for an over-actuated triangular floating platform," in *2014 IEEE Conference on Control Applications (CCA)*, 2014, pp. 891–896.
- [18] K. Tziortziotis, K. Vlachos, and K. Blekas, "Reinforcement learning-based motion planning of a triangular floating platform under environmental disturbances," in *2016 24th Mediterranean Conference on Control and Automation (MED)*, 2016, pp. 1014–1019.
- [19] T. Fossen, *Handbook of Marine Craft Hydrodynamics and Motion Control*, 05 2011.
- [20] T. I. Fossen, "Guidance and control of ocean vehicles," 1994.
- [21] D. Mayne, J. Rawlings, C. Rao, and P. Scokaert, "Constrained model predictive control: Stability and optimality," *Automatica*, vol. 36, no. 6, pp. 789–814, 2000. [Online]. Available: <https://www.sciencedirect.com/science/article/pii/S0005109899002149>
- [22] J. Zeng, Z. Li, and K. Sreenath, "Enhancing feasibility and safety of nonlinear model predictive control with discrete-time control barrier functions," 2021. [Online]. Available: <https://arxiv.org/abs/2105.10596>
- [23] J. A. E. Andersson, J. Gillis, G. Horn, J. B. Rawlings, and M. Diehl, "CasADi – A software framework for nonlinear optimization and optimal control," *Mathematical Programming Computation*, vol. 11, no. 1, pp. 1–36, 2019.
- [24] A. Wächter and L. Biegler, "On the implementation of an interior-point filter line-search algorithm for large-scale nonlinear programming," *Mathematical programming*, vol. 106, pp. 25–57, 03 2006.